A MODEL FOR THE COMPLEX PERMITTIVITY OF WATER AT FREQUENCIES BELOW 1 THz

Hans J. Liebe, George A. Hufford, and Takeshi Manabe

International Journal of Infrared and Millimeter Waves, Vol. 12, No. 7, 1991

A MODEL FOR THE COMPLEX PERMITTIVITY OF WATER AT FREQUENCIES BELOW 1 THz

Hans J. Liebe, George A. Hufford, and Takeshi Manabe[1]

National Telecommunications and Information Administration
Institute for Telecommunication Sciences
Boulder, Colorado 80303-3328

Received April 6, 1991

Experimental permittivity data of liquid water, compiled from the open literature, were selectively applied to support a modeling strategy. Frequencies up to 1 THz and atmospheric temperatures are covered with an expression made up by two relaxation (Debye) terms. The double-Debye model reduces to one term when the high frequency limit is set at 100 GHz, and the model can be extended to 30 THz by adding two resonance (Lorentzian) terms. The scheme was carried out by employing nonlinear least-squares fitting routines to data we considered reliable.

1. Introduction

A need was recognized for a physical model describing the permittivity of liquid water for the near-millimeter-wave range (NMW: 0.1 - 1 THz) at atmospheric temperatures. In this paper, we update our initial results and give a detailed account of the modeling strategy [1]. Dielectric properties of water plays a key role in computations of atmospheric propagation and remote sensing effects caused by rain drops and by droplets suspended in fogs or clouds [2]. Other effects considered in propagation models relate to molecular absorption by line (H_2O, O_2) and continuum (H_2O, N_2) spectra [3]. With respect to system operations in inclement weather, NMW signals experience much less loss than infrared/optical signals. A reliable model is useful to compute the advantage.

[1] T. Manabe was with the Institute for Telecommunication Sciences, NTIA-DoC, on leave from the Radio Research Laboratory, Ministry of Posts and Telecommunications, Koganei, Tokyo 184. He is now with ATR Optical and Radio Communications Research Laboratories, Seika-cho, Soraku-gun, Kyoto 619-02, Japan.

0195-9271/91/0700-0659$06.50/0

The empirical broadband model by *Ray* [4] has been a standard when it comes to predict dielectric properties of water. His model is divided into seven spectral ranges ($0 \leq f \leq 300$ THz), of which the first four extend to 30 THz. More than 30 coefficients are needed to support this part of the model. Because of considerable new experimental evidence since 1972, it was felt that an update of the Ray model was in order.

The paper is organized in five sections. Following the introduction, the interaction mechanisms between electromagnetic waves and liquid water are introduced (Sect. 2); then the published data are reviewed for their suitability to support a specific model (Sect. 3). Spectral models for the complex permittivity that fit best the selected data are detailed in Section 4, followed by a discussion of uncertainty estimates for the proposed prediction schemes.

2. Dielectric Spectral Properties of Water

The relative dielectric constant of water is referred to as complex permittivity,

$$\epsilon = \epsilon' + i\epsilon'',$$

where ϵ' and ϵ'' are real and loss parts, and $i = \sqrt{-1}$. The functional dependence of $\epsilon(f,T)$ on frequency f and temperature T reveals information on the interaction mechanism between EM radiation and H_2O molecules forming a liquid. Two distinct processes, namely relaxation and resonance behavior, may be recognized [5],[6].

The frequency dependence of the permittivity of pure water is given by the well-known Debye equation or its modification by Cole-Cole. Up to about 100 GHz, the simpler Debye model proved to be adequate to describe $\epsilon(f)$ [7],[13]. Resonance phenomena due to intra- and inter-molecular vibrations determine the frequency behavior in the infrared range (≥ 1 THz), where spectral functions with a Lorentzian or Gaussian shape have been considered. In the transition from 0.1 to 1 THz there is conflicting evidence, which has been interpreted either as a second relaxation process (possibly due to free H_2O molecules within the liquid quasi-lattice) [8] or as a weak resonance centered at 1.5 THz [9].

This work had three main objectives: (a) To formulate a model for the spectral dependence of the permittivity $\epsilon(f)$ that is valid for frequencies up to 1 THz; (b) to determine a temperature dependence for the salient model parameters; and (c) to estimate the prediction uncertainties. By selecting suitable functions for $\epsilon(f,T)$ to fit the experimental data, the effort was also directed to come up with simpler, more accurate formulations than those given by *Ray* [4].

3. Complex Permittivity Data

Below 100 GHz, the Debye relaxation model describes the permittivity spectrum of water with three temperature-dependent parameters. At higher frequencies, additional relaxation and resonance terms have to be considered. When the frequency range was extended to 1 THz, the reported experimental data were found deficient in both quality and quantity. To provide some confidence on how to bridge the spectral gap from 0.1 to 1 THz, we extended the range of frequencies up to 30 THz.

3.1 Static Dielectric Constant

The static dielectric constant ϵ_o of pure water depends on temperature. Representative values (32×), reported over a wide span of temperatures (-20° ≤ T ≤ 60°C), were least-squares fitted to the simple expression

$$\epsilon_o(T) = 77.66 - 103.3 \cdot \theta. \tag{1}$$

To express temperature dependence, a modified relative inverse variable,

$$\theta = 1 - 300/[273.15 + T(°C)],$$

was adopted from MPM [3], which changes for T ≈ 0 to 40°C from $\theta \approx$ -0.1 to 0.04. The excellent fit [$\sigma_\epsilon = 0.12$, see (8)] of the published data by (1) is demonstrated in Figure 1.

3.2 The Spectral Range Below 1 THz

The Debye shape,

$$\epsilon_D(f) = (\epsilon_o - \epsilon_\infty)/[1 - i(f/\gamma_D)] + \epsilon_\infty\ , \tag{2}$$

is a starting point for discussions on the frequency dependence of the complex permittivity of water. *Kaatze and Uhlendorf* applied a nonlinear regression analysis to over 380 complex data of $\epsilon_x(f,T)$ [7]. They confirmed (2) at frequencies from 0.1 to 114 GHz for nine temperature groups (-4 to 40°C) and list the values for the high-frequency constant ϵ_∞ ($f \to \infty$) and the relaxation frequency $\gamma_D = 1/2\pi\tau$ (τ = relaxation time constant).

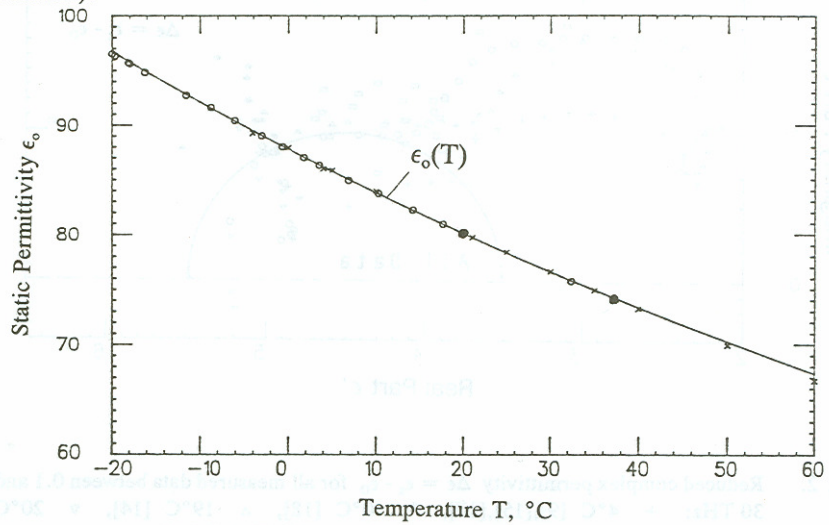

Fig. 1. Static dielectric constant ϵ_o of pure water over the temperature range from -20° to 60°C: — Eqn (1); × [7], ○ [10], • [13].

To begin, the values of ϵ_o, ϵ_∞, and γ_D from reference [7] were substituted into the Debye function (2) to compute the first 33 data entries of Table I(*a*). These quasi-data represented the permittivity for frequencies below 100 GHz. To extend the frequency range above 100 GHz, first all data measured up to 30 THz (Ref. [14] through [21]) were reduced by subtracting the Debye contribution ϵ_D (2). The reduced results $\Delta\epsilon$ are shown in Figure 2 to illuminate the fitting problem at hand.

The selection of reliable NMW data was trying. Measurement techniques are far from being perfect and reported experimental values of $\epsilon_x(f,T)$ were sparse and usually without quoted experimental errors. Several data sets appear to be biased by systematic errors. The graphical array in the complex plane provided some guidance for the probable trend suggested by the overall data body. In such a plot, Debye relaxation (single characteristic frequency) displays a semicircular arc, Cole-Cole relaxation (spread of characteristic frequencies) models $\epsilon(f)$ as an elliptical arc, and overlapping resonances appear in circular loops. An additional Debye term and two, overlapping resonances were recognized in the $\Delta\epsilon$ data.

The permittivity data which represent the range below 1 THz are listed in Table I. Primary Debye relaxation behavior displays in the complex plane a semicircular arc. Results at four temperatures are plotted in Figure 3. Fits of the NMW characteristics improved noticeably when a second Debye term was considered. The enlarged curve of the complex permittivity $\epsilon(f,T)$ in Figure 4 reveals the results. Details of the double Debye model (4) are discussed in Sect. 4.3.

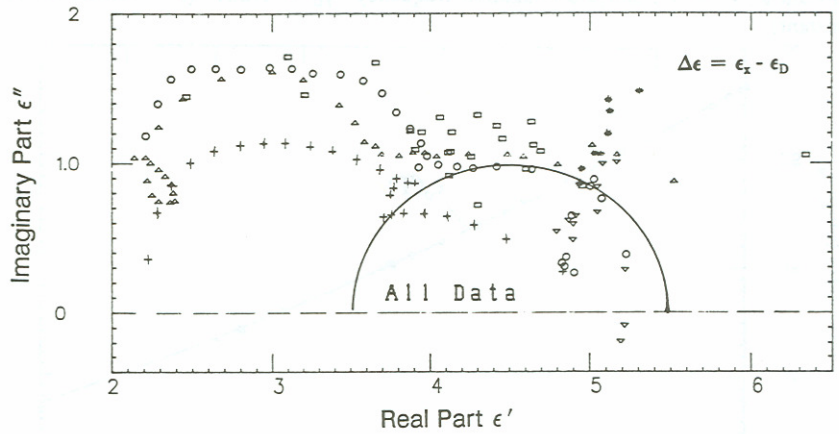

Fig. 2. Reduced complex permittivity $\Delta\epsilon = \epsilon_x - \epsilon_D$ for all measured data between 0.1 and 30 THz: + 4°C [9],[15],[17], * 10°C [18], △ 19°C [14], ▽ 20°C [18], □ 25°C [16],[20], ○ 30°C [9],[15],[17],[18];
—— possible locus of a second Debye function.

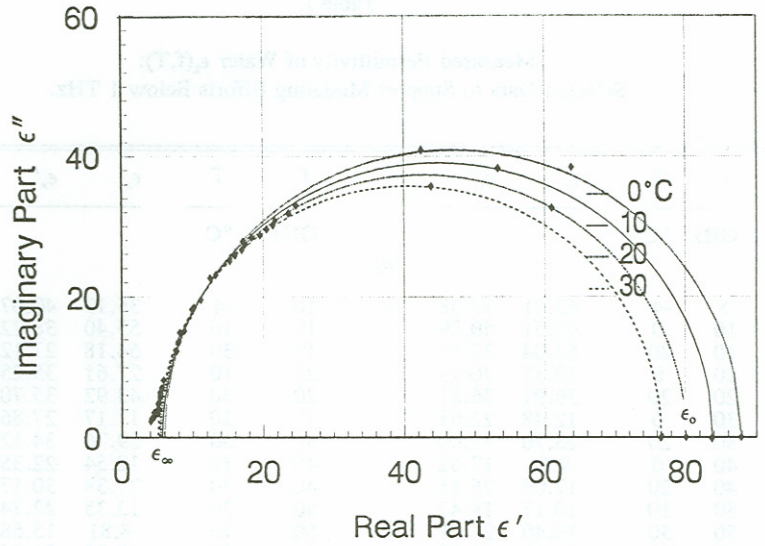

Fig. 3. The complex permittivity $\epsilon(f,T)$ of water below 0.1 THz:
—— Single Debye (2), ◆ - Table I and [13].

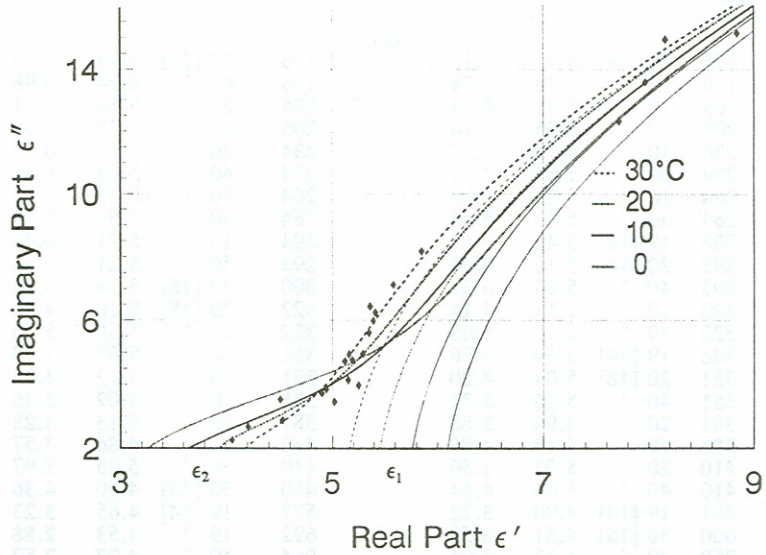

Fig. 4. The complex permittivity $\epsilon(T,f)$ of water between 0.1 and 1 THz:
— Double Debye (4), --- Eqn (2), see Fig.3; ◆ - Table I.

Table I.

Measured Permittivity of Water $\epsilon_x(f,T)$:
Selected Data to Support Modeling Efforts Below 1 THz.

f	T	ϵ_x'	ϵ_x''		f	T	ϵ_x'	ϵ_x''
GHz	°C				GHz	°C		
				(a)				
5	-4	63.81	38.38	[7]	10	-4	36.13	40.07
10	0	42.51	40.89		10	10	53.40	38.22
10	20	61.04	32.59		10	30	64.18	27.12
20	0	19.55	30.79		20	10	27.61	35.25
20	20	36.91	36.81		20	30	43.92	35.70
30	0	12.48	22.65		30	10	17.17	27.86
30	20	23.76	32.00		30	30	29.76	34.12
40	0	9.65	17.62		40	10	12.54	22.35
40	20	17.04	26.85		40	30	21.38	30.17
50	10	10.17	18.47		50	20	13.35	22.74
50	30	16.40	26.31		60	10	8.81	15.68
60	20	11.17	19.57		60	30	13.29	23.06
70	10	7.97	13.59		70	20	9.78	17.11
70	30	11.26	20.40		80	20	8.84	15.17
80	30	9.87	18.23		90	20	8.19	13.61
90	30	8.88	16.44		100	20	7.72	12.33
100	30	8.16	14.96					
				(b)				
176	10 [18]	5.71	7.10		176	20 [18]	5.73	7.79
176	30 "	6.28	8.99		176	40 "	6.24	9.98
205	10	5.41	8.24		205	20	5.58	7.11
205	30	5.85	8.16		205	40	5.78	9.00
234	10	5.35	5.57		234	20	5.55	6.37
234	30	5.60	7.34		234	40	5.68	8.16
264	10	5.29	4.95		264	20	5.35	5.61
264	30 "	5.36	6.43		264	40	5.51	7.19
288	19 [14]	5.42	5.42		293	10	5.21	4.44
293	20 [18]	5.16	4.94		293	30 "	5.21	5.54
293	40 "	5.34	6.32		300	30 [15]	5.39	5.98
322	10	5.15	4.14		322	20 [18]	5.10	4.50
322	30 "	5.16	5.05		322	40 "	5.30	5.76
346	19 [14]	5.19	4.76		351	10	5.05	3.78
351	20 [18]	5.04	4.20		351	30	5.12	4.72
351	40 "	5.26	5.32		381	10	5.02	3.46
381	20	4.94	3.85		381	30	5.13	4.28
381	40	5.16	4.88		410	10	4.86	3.57
410	20	5.02	3.56		410	30 "	5.25	3.97
410	40 "	5.04	4.54		450	30 [15]	4.80	4.36
461	19 [14]	4.90	3.72		577	19 [14]	4.65	3.23
600	30 [15]	4.51	3.53		692	19 "	4.53	2.88
750	30 "	4.33	3.01		864	19 "	4.27	2.52
900	30 "	4.21	2.68		1038	19 "	4.06	2.26
1050	30 "	4.08	2.45					

3.3 Far-Infrared Range (≤ 30 THz)

At frequencies above 1 THz, absorption bands due to resonance processes become important while the relaxation contributions vanish [5],[6]. The selected data are given in Table II. A minimum in the loss part ϵ'' marks the transition from Debye to resonance behavior at 2.5 THz. The locus of the selected data ϵ_x is plotted in Figure 5 and reveals two, overlapping resonances. The data have relatively small uncertainties (≤ 5%) reported and are consistent from 1 to 30 THz.

In summary, the model-supporting data are listed in Tables I and II. Scanning the tables, one notices that we relied foremost on four studies [7],[18],[19],[20], while the following data sets are included in Figure 2, but were rejected for fitting purposes:

f ≤ 1 THz	[9],[17]	T = 4° to 30°C,
f ≤ 6.3 THz	[15]	T = 4° and 30°C,
f ≤ 5.3 THz	[16]	T = 25°C,
9.8 THz ≤ f	[20]	T = 25°C.

These sets seemed not compatible with the general trend. Discrepancies of several standard deviations were recognized among values obtained by different groups. Our subjective judgement on which data to refuse and how to bridge spectral blanks remains a source of concern when it comes to perform a rigorous error analysis (see Sect. 5).

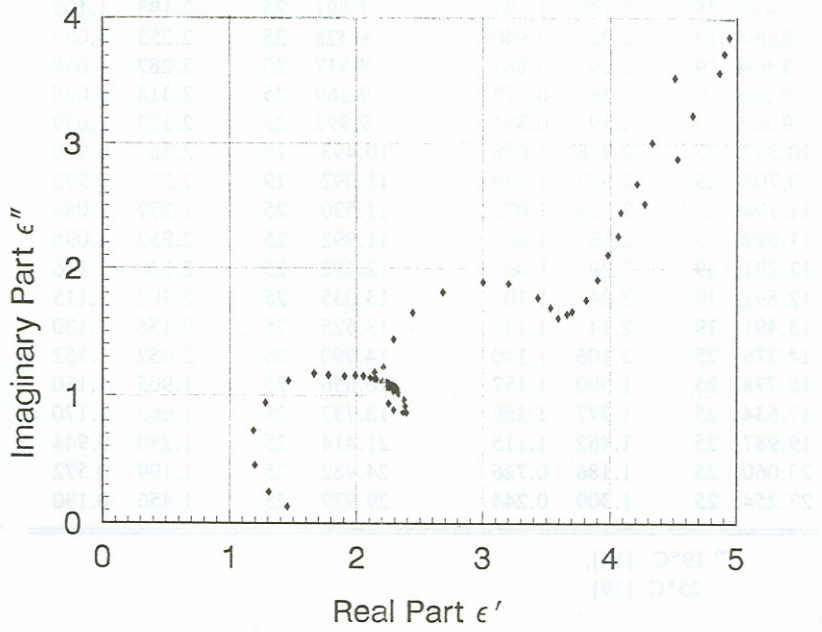

Fig. 5. Selected complex permittivity data ϵ_x between 1 and 30 THz: ◆ - Table II.

Table II.

Measured Permittivity of Water $\epsilon_x(f,T)$:
Selected Data to Support Modeling Efforts Between 1 and 30 THz

f	T*)	ϵ_x'	ϵ_x''	f	T*)	ϵ_x'	ϵ_x''
THz	°C			THz	°C		
1.038	19	4.06	2.26	1.211	19	3.98	2.11
1.499	19	3.90	1.91	1.799	19	3.81	1.75
2.099	19	3.70	1.66	2.398	19	3.66	1.64
2.698	19	3.59	1.61	2.998	19	3.53	1.69
3.298	19	3.43	1.77	3.897	19	3.20	1.88
4.497	19	3.00	1.89	5.096	19	2.68	1.81
5.696	19	2.44	1.65	6.296	19	2.29	1.44
6.895	19	2.21	1.22	7.495	19	2.22	1.05
7.495	25	2.140	1.181	7.891	25	2.198	1.105
8.094	19	2.25	0.940	8.328	25	2.253	1.063
8.694	19	2.29	0.887	8.817	25	2.287	1.038
9.294	19	2.36	0.872	9.369	25	2.318	1.028
9.893	19	2.39	0.874	9.992	25	2.323	1.039
10.337	25	2.318	1.048	10.493	19	2.38	0.920
10.706	25	2.312	1.059	11.092	19	2.37	0.972
11.104	25	2.299	1.073	11.530	25	2.277	1.084
11.692	19	2.33	1.02	11.992	25	2.252	1.095
12.291	19	2.29	1.06	12.492	25	2.230	1.106
12.891	19	2.24	1.10	13.035	25	2.202	1.115
13.491	19	2.14	1.13	13.625	25	2.156	1.130
14.276	25	2.106	1.140	14.990	25	2.052	1.152
15.778	25	1.990	1.157	16.656	25	1.905	1.150
17.634	25	1.777	1.159	18.737	25	1.665	1.170
19.987	25	1.462	1.115	21.414	25	1.280	0.944
23.060	25	1.186	0.726	24.982	25	1.199	0.572
27.254	25	1.309	0.244	29.979	25	1.456	0.130

*) 19°C [14],
25°C [19]

4. Spectral Models for the Complex Permittivity of Water

The formulation of a reliable complex permittivity model of pure water, $\epsilon(f,T)$, for applications in atmospheric propagation at frequencies up to 1 THz was the main objective of this study [1].

4.1. Single Debye Model

The single Debye model ϵ_D (2) has been verified by many researchers (e.g., [7],[11] through [13]) as correct description of experimental data below 100 GHz. Polynomial expressions provided a best fit to the temperature dependence of the relaxation frequency γ_D and the high-frequency constant ϵ_∞ [1].

Fitting the data of Table I(a) with (2) resulted in [$\sigma_D = 0.18$, see (8)]

$$\epsilon_\infty = 0.066 \cdot \epsilon_o \,,$$

and (2a)

$$\gamma_D = 20.27 + 146.5 \cdot \theta + 314 \cdot \theta^2 \quad \text{GHz.}$$

The Debye parameters ϵ_o and ϵ_∞ decrease with temperature in the same manner. Accurate measurements at frequencies from 29 to 45 GHz at 20 and 37°C by *Alison and Sheppard* confirmed this model [13]. Figure 3 displays the complex plane for ϵ_D at four temperatures.

Water becomes less viscous as the temperature increases. Theory conjectures that hydrogen-bonded friction forces between H_2O molecules follow an exponential temperature law [6]. Such assumption leads with the same data to an alternate, though less reliable [$\sigma_\gamma = 0.28$ vs 0.05 GHz, see (8)] fit of the relaxation frequency,

$$\gamma_D^* = 20.1 \exp(7.88 \cdot \theta) \quad \text{GHz.} \tag{2b}$$

Single Debye Behavior at NMW Frequencies:

At frequencies between 176 and 410 GHz, the experimental permittivities ϵ_x reported by *Hasted* et al. [18] deviate from the single Debye model (2); i.e., real parts ϵ' are predicted too high and losses ϵ'' too low. It is interesting to note that this limited data set (36 frequencies, 10-40°C) provided a best fit [$\sigma_\epsilon = 0.22$, $\sigma_\gamma = 0.16$ GHz, see (8)] to a Debye model with

$$\epsilon_{\infty,m} = 4.83 + 1.4 \cdot \theta$$

and (3)

$$\gamma_{D,m} = 22.1 \exp(4.99 \cdot \theta) \quad \text{GHz.}$$

The temperature dependence of these Debye parameters is quite different from (2).

4.2. Double Debye Model

Extending the spectral range of $\epsilon(f,T)$ beyond 100 GHz leads to the problem of how to merge the conflicting results [i.e., (2) vs. (3)] into one continuous spectrum. When all data of Table I were fitted to (2), the values of ϵ_∞ and γ_D changed very little, but the standard deviation of the overall fit increased three times, indicating that additional polarization mechanisms come into play.

Different fitting schemes were tried using Debye, Cole-Cole, and mixed (Debye + Lorentzian) formulations with polynomial or exponential temperature dependences of the parameters. Assuming that $\epsilon_o(T)$ is given by (1), we experimented with about twenty different 5-6-7-8-9-parameter combinations to fit the $\epsilon_x(f,T)$ data of Table I. The most satisfactory fit [$\sigma_M = 0.21$, (8)] was provided by the following 7-parameter double Debye model:

$$\epsilon_M(f) = (\epsilon_o - \epsilon_1)/[1 - i(f/\gamma_1)] + (\epsilon_1 - \epsilon_2)/[1 - i(f/\gamma_2)] + \epsilon_2$$
$$= \epsilon_o - f\,[(\epsilon_o - \epsilon_1)/(f + i\gamma_1) + (\epsilon_1 - \epsilon_2)/(f + i\gamma_2)], \tag{4}$$

where

$$\epsilon_1 = 0.0671\cdot\epsilon_o\,, \tag{4a}$$
$$\gamma_1 = 20.20 + 146.4\cdot\theta + 316\cdot\theta^2 \quad \text{GHz},$$

and

$$\epsilon_2 = 3.52 + 7.52\cdot\theta, \tag{4b}$$
$$\gamma_2 = 39.8\gamma_1\,.$$

First and second high-frequency constants are labled ϵ_1 , ϵ_2 ; and γ_1 , γ_2 denote primary and secondary relaxation frequencies. The principal Debye parameters did not change much ($\epsilon_1 \approx \epsilon_\infty$, $\gamma_1 \approx \gamma_D$). Figure 4 displays the complex plane for ϵ_M at 0-10-20-30 °C.

Upon rationalizing (4), the expressions for real and imaginary parts are

$$\epsilon_M' = (\epsilon_o - \epsilon_1)/[1 + (f/\gamma_1)^2] + (\epsilon_1 - \epsilon_2)/[1 + (f/\gamma_2)^2] + \epsilon_2$$

and

$$\epsilon_M'' = (\epsilon_o - \epsilon_1)(f/\gamma_1)/[1 + (f/\gamma_1)^2] + (\epsilon_1 - \epsilon_2)(f/\gamma_2)/[1 + (f/\gamma_2)^2]. \tag{5}$$

Examples of spectra $\epsilon_M'(f,T)$ and $\epsilon_M''(f,T)$ from 2 GHz to 2 THz are exhibited in Figure 6. Contributions from the principal relaxation can be isolated by setting $\epsilon_2 = \epsilon_1$.

4.3. Broadband Model

The extension into the far-infrared frequency range was modeled by retaining the double Debye model (4) and supplementing it with two Lorentzian resonance terms. The selected resonance data set is listed in Table II and the complex values are plotted in Figure 5. The data were fitted to the resonance model (f = 1 to 30 THz),

$$\epsilon_R = \sum_{r=1}^{2} [A_r/(f_r^2 - f^2 - i\gamma_r f) - A_r/f_r^2]\,. \tag{6}$$

The zero-frequency contributions A_r/f_r^2 are subtracted since they are implicitly in ϵ_2 (4b). Values for center frequency f_r , width γ_r , and strength A_r are given below:

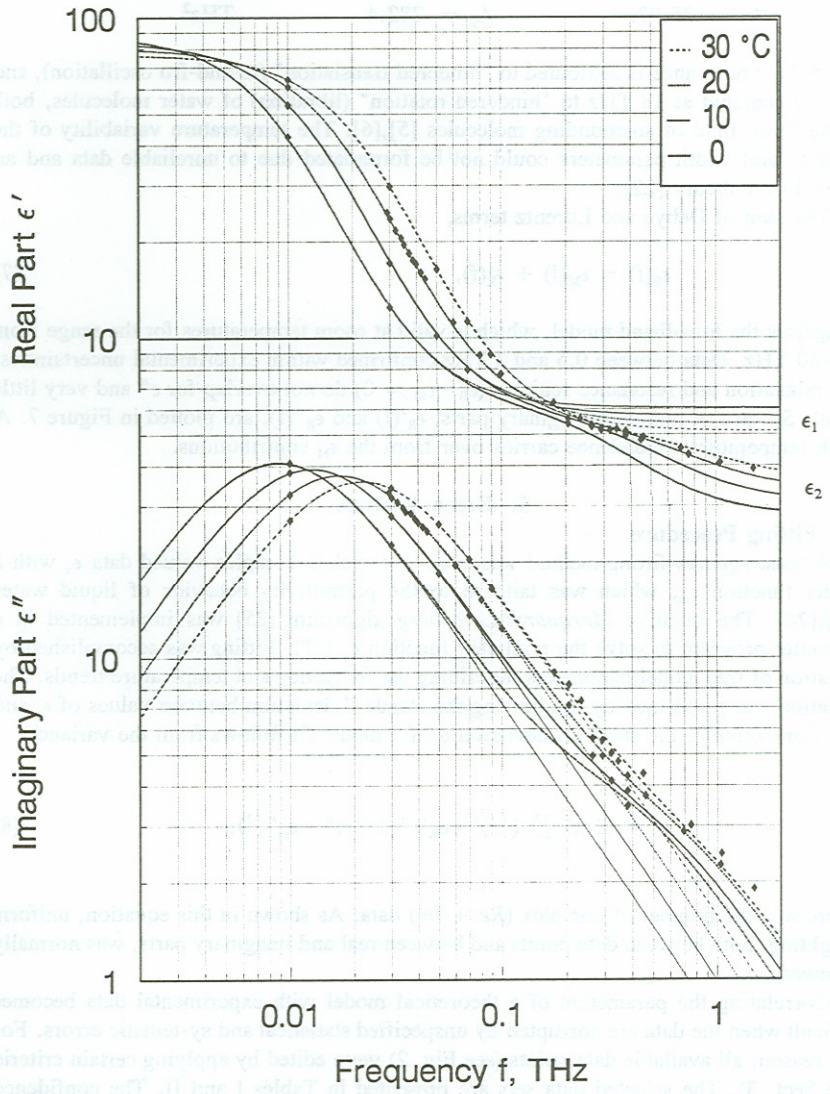

Fig. 6. Spectra of real (ϵ_M') and imaginary (ϵ_M'') parts of the permittivity of water from 2 GHz to 2 THz: — Eqn (4), -- Eqn (2); ◆ - Table I and [13].

$$\begin{aligned} f_1 &= 5.11, & f_2 &= 18.2 & &\text{THz}, \\ \gamma_1 &= 4.46, & \gamma_2 &= 15.4 & &\text{THz}, \\ A_1 &= 25.03, & A_2 &= 282.4 & &\text{THz}^2. \end{aligned} \tag{6a}$$

The 5-THz resonance is attributed to "hindered translation" (to-and-fro oscillation), and the one centered at 18 THz to "hindered rotation" (libration) of water molecules, both in the force field of surrounding molecules [5],[6]. The temperature variability of the strength and width parameters could not be formulated due to unreliable data and an inconclusive theory [22].

The sum of Debye and Lorentz terms,

$$\epsilon_B(f) = \epsilon_M(f) + \epsilon_R(f), \tag{7}$$

comprises the broadband model, which is valid at room temperatures for the range from 0 to 30 THz. Data between 0.5 and 1 THz confirmed within experimental uncertainties, that relaxation and resonance regimes ($\epsilon_B - \epsilon_M \approx 0$) do not overlap for ϵ'' and very little for ϵ'. Spectra of real and imaginary parts, $\epsilon_B'(f)$ and $\epsilon_B''(f)$, are plotted in Figure 7. A weak temperature dependence carries over from the ϵ_M contributions.

5. Error Analysis

5.1 Fitting Procedure

A least squares fitting method was used to correlate complex-valued data ϵ_x with a model function ϵ_m, which was tailored to the permittivity behavior of liquid water [23],[24]. The iterative *Marquardt-Levenberg* algorithm [25] was implemented in a computer program to solve the nonlinear function $\epsilon_m(f,T)$. Fitting was accomplished by variation of free model parameters describing the frequency and temperature trends. The variation was performed by minimizing the standard deviation between values of ϵ_x and ϵ_m . For example, the standard deviation σ of a model-fit follows from the variance

$$\sigma^2 = (1/n) \sum_n \left(|\epsilon_x' - \epsilon_m'|^2 + |\epsilon_x'' - \epsilon_m''|^2 \right), \tag{8}$$

where n is the number of complex (*Re* + *Im*) data. As shown in this equation, uniform weighting, both between data points and between real and imaginary parts, was normally followed.

Correlating the parameters of a theoretical model with experimental data becomes difficult when the data are corrupted by unspecified statistical and systematic errors. For that reason, all available data points (see Fig. 2) were edited by applying certain criteria (see Sect. 3). The selected data sets are presented in Tables I and II. The confidence level of a model to predict these data is expressed by a standard deviation, which only has a quantitative physical meaning (i.e., absolute error bound) when the systematic errors are known. However, it is an advantage to have simple analytical expressions that yield good agreement with the tabulated values since individual values of $\epsilon_x(f,T)$ are not particular convenient for computational purposes [26].

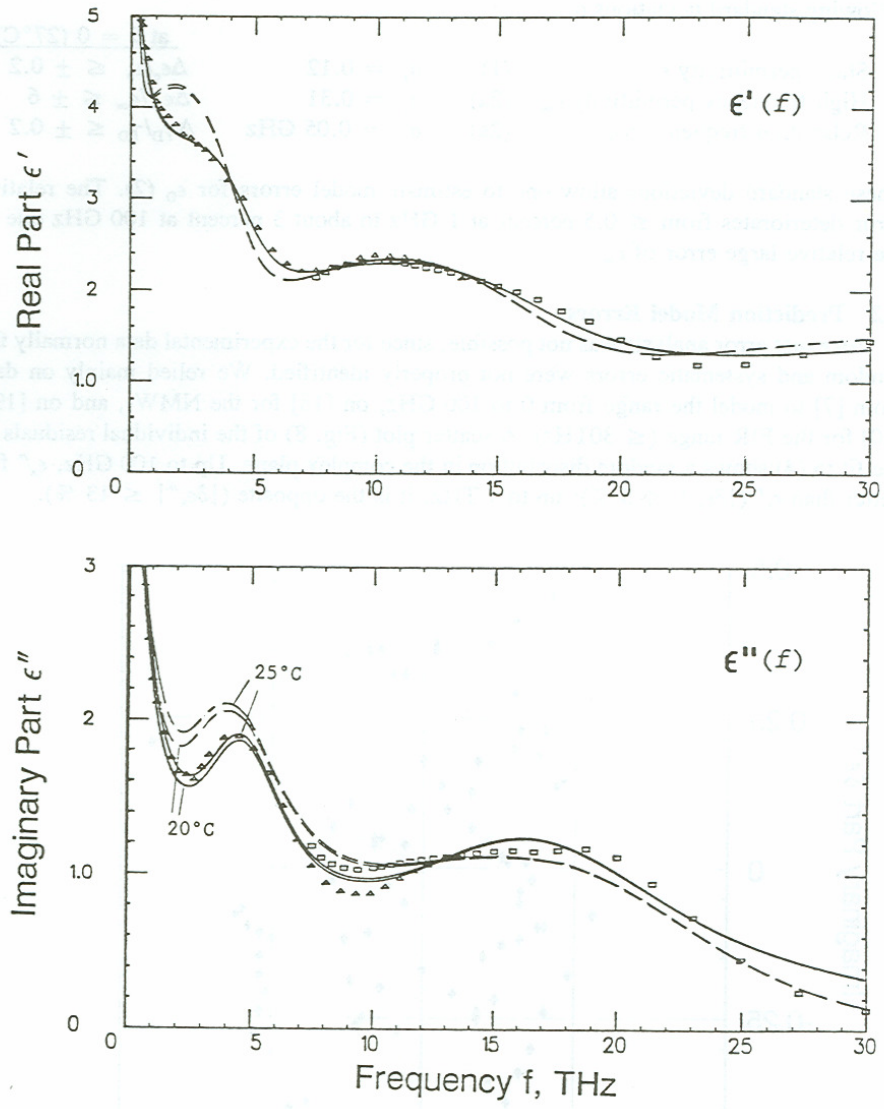

Fig. 7. Spectra $\epsilon'(f)$ and $\epsilon''(f)$ of the permittivity of water up to 30 THz:
—— Eqn (7), - - Ray model [4]; △ [11], □ [15].

5.1 Debye Parameter Errors

Fits to a temperature function for reported individual Debye parameters provided the following standard deviations σ:

			at θ = 0 (27°C)
• Static permittivity ϵ_o	(1)	σ_ϵ = 0.12	$\Delta\epsilon_o/\epsilon_o \leq \pm$ 0.2 %
• High-frequency permittivity ϵ_∞	(2a)	σ_ϵ = 0.31	$\Delta\epsilon_\infty/\epsilon_\infty \leq \pm$ 6 %
• Relaxation frequency γ_D	(2a)	σ_γ = 0.05 GHz	$\Delta\gamma_D/\gamma_D \leq \pm$ 0.2 %

These standard deviations allow one to estimate model errors for ϵ_D (2). The relative error deteriorates from $\leq$ 0.5 percent at 1 GHz to about 3 percent at 100 GHz due to the relative large error of ϵ_∞ .

5.2 Prediction Model Errors

An exact error analysis was not possible, since for the experimental data normally the random and systematic errors were not properly identified. We relied mainly on data from [7] to model the range from 0 to 100 GHz, on [18] for the NMW-, and on [19], [20] for the FIR-range ($\leq$ 30THz). A scatter plot (Fig. 8) of the individual residuals of the fit to (4) shows a random distribution in the complex plane. Up to 100 GHz, ϵ_x'' fits better than ϵ_x' ($|\delta\epsilon_x'| \leq 5$ %); up to 1 THz, it is the opposite ($|\delta\epsilon_x''| \leq 13$ %).

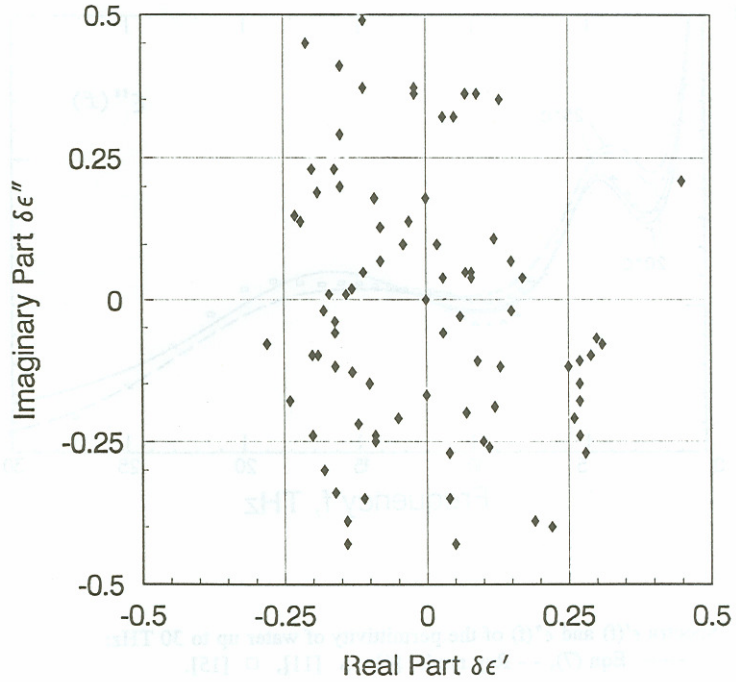

Fig. 8. Residuals $\delta\epsilon_M = \epsilon_x - \epsilon_M$ of the fit to model (4) for the data of Table I.

Three permittivity models evolved from fits of ϵ_x-data:

Model	Eqn	Data Set (Table)	Overall Fitting Uncertainty σ_m	σ_{Ray}	Estimated Maximum Prediction Error $\lvert\Delta\epsilon_m\rvert$ (%)
ϵ_D	(2)	I(*a*)	0.18	0.60	3
ϵ_M	(4)	I	**0.21**	0.65	10
ϵ_R	(6)	II	0.10	0.25	5

Individual residuals $\delta\epsilon = \epsilon_x - \epsilon_m$ for real and imaginary parts are plotted in Fig. 9. The prediction uncertainty of an ϵ-model is expressed by the overall standard deviation σ_m (8); the same data set led to σ_{Ray} when analyzed with the Ray model [1].

The absolute accuracy $\lvert\Delta\epsilon\rvert$ of model predictions was estimated to be better than 3 percent below 100 GHz and on the order of 10 percent at higher frequencies, both adequate for the intended MPM applications. Fitting uncertainties for the data (Tables I,II) are in each case much improved over the Ray model.

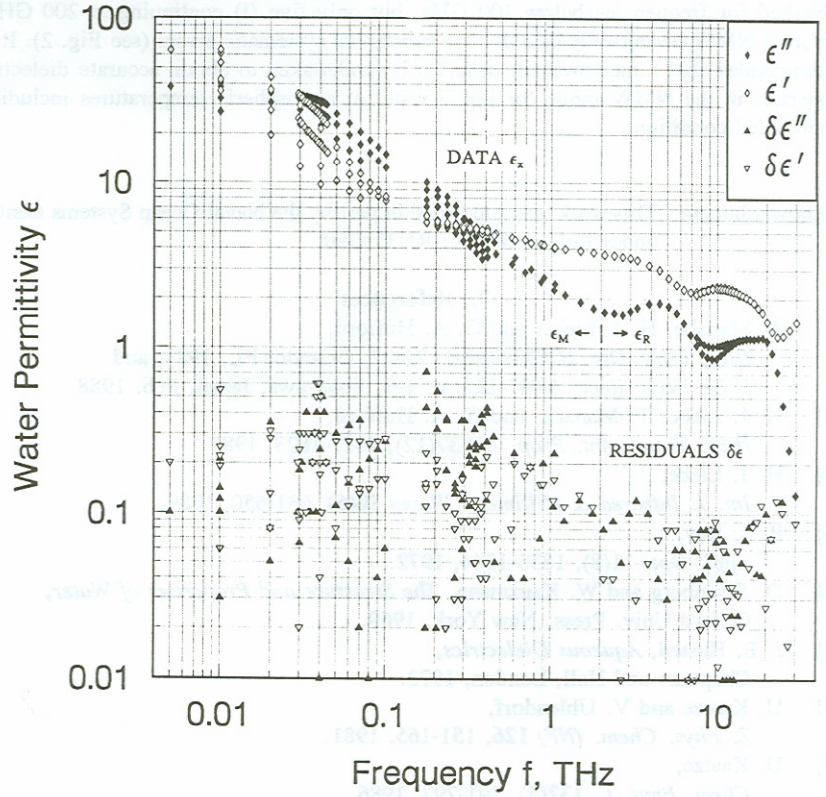

Fig. 9. Permittivity data ϵ_x (Tables I, II) and the residuals $\lvert\delta\epsilon\rvert = \epsilon_x - \epsilon_{M,R}$.

6. Conclusions

Dielectric properties of pure water for the spectral range from 0 to 1 THz are described by the double Debye model (4), which for room temperatures is extended up to 30 THz by the resonance model (7). Each model predicts measured permittivity data ϵ_x more accurately and in simpler fashion (less than half the number of parameters) than the Ray model [4]. The single Debye model (2), which is supported by a large body of data, is included in model (4), the center piece of this effort. Expression (4) is a *best* fit to the data collected in Table I; and the spectral extension to 30 THz with (6) blends smoothly with the Debye formulation. The transition from relaxation to predominantly resonance processes happens around 2.5 THz. A weak resonance, presumed to be centered around 1.5 THz [8], could not be confirmed.

The practical value of the new NMW permittivity model for water is succinctly illustrated by an example: At 400 GHz and 10°C, a cloud or fog with 0.1 g/m^3 liquid water droplet content ($\approx$ 300 m visibility) have with the *new* model (4) a predicted attenuation rate of $\alpha = 1.9$ dB/km, while at that frequency the outmoded Debye model (2) predicts little more than half (1.1 dB/km) [2].

Numerous ($>$ 400) complex permittivity data $\epsilon_x(f,T)$ on pure water have been published for frequencies below 100 GHz, but only five (!) continuing to 200 GHz. Reported NMW permittivity data display substantial systematic errors (see Fig. 2). It is recommended that a measurement program be undertaken to obtain accurate dielectric properties in the NMW range for liquid water at atmospheric temperatures including supercooled conditions.

Acknowledgment: This work was supported in part by the Naval Ocean Systems Center under Reference No.: RU35 G80.

7. References

[1] T. Manabe, H. J. Liebe, and G. A. Hufford,
IEEE Conf. Dig. **87CH1490**-1, 21-22, Orlando, FL, 1987; and
IECE Tech. Rept. **AP87-121**, p. 1-6; Yonezawa, Japan, Feb. 1988.

[2] H. J. Liebe, T. Manabe, and G. A. Hufford,
IEEE Trans. Ant. Prop. **AP-37**(12), 1617-1623, 1989.

[3] H. J. Liebe,
Int. J. Infrared & Millimeter Waves **10**(6), 631-650, 1989.

[4] P. S. Ray,
Appl. Opt. **11**(8), 1836-1844, 1972.

[5] D. Eisenberg and W. Kauzmann, *The Structure and Properties of Water*,
Oxford Univ. Press, New York, 1969.

[6] J. B. Hasted, *Aqueous Dielectrics*,
Chapman and Hall, London, 1973.

[7] U. Kaatze and V. Uhlendorf,
Z. Phys. Chem. (NF) **126**, 151-165, 1981.

[8] U. Kaatze,
Chem. Phys. L. **132**(3), 291-293, 1986.

[9] J. B. Hasted, S. K. Husain, F. A. Frescura, and J. R. Birch,
Chem. Phys. L. **118**(6), 622-625, 1985.
[10] D. Bertolini, M. Cassettari, and G. Salvetti,
J. Chem. Phys. **76**(6), 3285-90, 1982.
[11] L. Zanforlin,
IEEE Trans. Microwave Theory Tech. **MTT-31**(5), 417-419, 1983.
[12] H. Zaghloul and H. A. Buckmaster,
J. Phys. D: Appl.Phys. **18**, 2109-18, 1985.
[13] J. M. Alison and R. J. Sheppard,
Meas. Sci. Technology **1**, 1093-98, 1990.
[14] M. N. Afsar and J. B. Hasted,
J. Opt. Soc. Am. **67**(7), 902-904, 1977.
[15] M. N. Afsar and J. B. Hasted,
Infrared Phys. **18**, 835-841, 1978.
[16] O. A. Simpson, B. L. Bean, and S. Perkowitz,
J. Opt. Soc. Am. **69**(12), 1723-26, 1979.
[17] M. D. Blue,
J. Geophys. Res. **85**(C2), 1101-06, 1980.
[18] J. B. Hasted, S. K. Husain, F. A. Frescura, and J. R. Birch,
Infrared Phys. **27**(1), 11-15, 1987.
[19] V. M. Zolotarev, B. A. Mikhailov, L. I. Alperovich, and S. L. Popov,
Opt. Spectr. **27**, 430-32, 1969.
[20] A. N. Rusk, D. Williams, and M. R. Querry,
J. Opt. Soc. Am. **61**(7), 895-903, 1971.
[21] J. K. Vij,
Int. J. Infrared & Millimeter Waves **10**(7), 847-867, 1989.
[22] G. M. Hale and M. R. Querry,
J. Opt. Soc. Am. **62**(9), 1103-08, 1972.
[23] R. J. Sheppard,
J. Phys. E: Sci. Instrum. **14**, 156-160, 1973.
[24] P. R. Mason, J. B. Hasted, and L. Moore,
Adv. Molec. Relax. Proces. **6**, 217-232, 1974.
[25] D. W. Marquardt,
J. Soc. Indust. Appl. Math. **11**(2), 431-441, 1963.
[26] A. Stogryn,
IEEE Trans. Microwave Theory Tech. **MTT-19**(8), 733-736, 1971.